IEEE Access
Multidisciplinary | Rapid Review | Open Access Journal

Received May 1, 2019, accepted May 25, 2019, date of publication May 29, 2019, date of current version June 11, 2019.

Digital Object Identifier 10.1109/ACCESS.2019.2919686

Design of Efficient LDPC Coded Non-Recursive CPE-Based GMSK System for Space Communications

HAI ZHU, (Member, IEEE), HENGZHOU XU, (Member, IEEE), BO ZHANG, MENGMENG XU, AND SIFENG ZHU

School of Network Engineering, Zhoukou Normal University, Zhoukou 466001, China

Corresponding author: Hengzhou Xu (hzxu@zknu.edu.cn)

This work was supported in part by the National Natural Science Foundation of China under Grant 61801527 and Grant 61103143, in part by the Training Program for Young Core Instructor of Henan Universities under Grant 2016GGJS-134 and Grant 2018GGJS137, in part by the Key Scientific Research Projects of Henan Educational Committee under Grant 19A510028 and Grant 18B510022, and in part by the Development Project of Henan Provincial Department of Science and Technology under Grant 192102210279, Grant 182102310867, Grant 182102310034, and Grant 182102210152.

ABSTRACT We consider a low-density parity-check (LDPC) coded non-recursive Gaussian minimum shift keying (GMSK) scheme for space communications subject to low signal-to-noise ratio (SNR), limited power, and spectrum resources. First, we design a non-recursive continuous-phase encoder (NRCPE)-based GMSK modulator to alleviate the impact of the error propagation existed in a recursive CPE (RCPE)-based one. Then, a corresponding pilot-aided quasi-coherent demodulation algorithm (PA-QCDA) is developed for improving the performance of the non-coherent demodulation and the impact of the Doppler shift in the coherent demodulation, whose basic principle is that a modified Bahl, Cocke, Jelinek, and Raviv (BCJR) algorithm-based detection performs on the received signals with initial and ending trellis-states being determined using the very small pilot overhead. Finally, we choose proper modulation parameters for the NRCPE-based GMSK signaling according to the tradeoffs between power and spectral efficiency. The simulation results show that the proposed system using the PA-QCDA can achieve excellent performance and can also work well in the presence of the large Doppler shifts and some burst errors.

INDEX TERMS LDPC, GMSK, BCJR, pilot-aided, space communications.

I. INTRODUCTION

In space communications such as deep space communications and satellite communications *etc.*, the transmission data links always work subject to the low signal-to-noise ratio (SNR), limited power and spectrum resources [1], [2]. As a class of constant envelope modulation technique with high spectral efficiency and power utilization, continuous phase modulation (CPM) can be a good choice for such communications [3]. Among CPM schemes, Gaussian minimum shift keying (GMSK) modulation [4], [5] is a very popular one due to the excellent bandwidth efficiency compared with binary phase shift keying (BPSK) and quadrature phase shift keying (QPSK), which has been adopted as a European standard for personal communication systems (PCSs) [2] and used in the European Space Agency (ESA) for deep-space missions [6]. Also, the GMSK modulation is more suitable for the high power amplifier (HPA) working in the saturation area than the quadrature amplitude modulation (QAM) and pulse position modulation (PPM).

In order to achieve higher coding gains in CPM systems, it is common to use forward error correction (FEC) code in conjunction with CPM. Some serially concatenated CPM (SCCPM) schemes were proposed in [7]–[9], where convolutional codes (CCs) are adopted with a joint iterative soft-in soft-out (SISO) decoder. Taking the advantages of space-time codes to combat channel fading and increase system capacity, the space-time coded CPM schemes were designed in [10]–[12]. Since low-density parity-check (LDPC) codes, proposed by Gallager in 1963 [13], were demonstrated to be capable of achieving near Shannon limit performance [14], some LDPC coded CPM schemes have also been considered in [15] and [16]. Furthermore, the combination method between the CPM modulations with the LDPC codes should

The associate editor coordinating the review of this manuscript and approving it for publication was Nan Wu.

mention another method, such as the coding part of the CPM, i.e., CPE (continuous-phase encoder), as part of the moderate or high rate extended irregular repeat and accumulated (eIRA) like LDPC codes [18], which can optimize the codes much better than the K. R. Narayanan's method [19]. In this paper, the introduced LDPC code can solve the problems of the low SNR and burst-error interference existed in space communications.

For any CPM modulator, Rimoldi has proved that it can be decomposed into a continuous-phase encoder (CPE) and a memoryless modulator (MM) [20], where the CPE has a recursive structure, i.e., its current phase state is related to all of previous input symbols. Thus, the so-called error propagation phenomenon will occur when the channel quality is not good. To solve this problem, we design a non-recursive CPE (NRCPE), whose output only depends on the current and previous L input symbols (L denotes the memory length). With the trellis representation the modulation process of the CPM using, the corresponding demodulation can be implemented by the classical BCJR (Bahl, Cocke, Jelinek and Raviv) algorithm [21]. At the receiver, the demodulation can be divided into the coherent demodulation and non-coherent demodulation, where the former can obtain excellent performance but with known channel state information (CSI); the latter is insensitive to the CSI but with poor performance.

In general, the known CSI is hard to be captured accurately such that the non-coherent demodulation is comparatively suitable for practical space communications but presenting non-negligible performance losses. Some solutions to the above performance losses have been proposed such as the optimal symbol-by-symbol detection, the multiple-symbol detection and the iterative SISO detection [22], [23]. However, these solutions have high complexity and processing latency. Thus, we propose a pilot-aided quasi-coherent demodulation algorithm (PA-QCDA) based on the sliding-window idea. Its basic principle is using the received signals in each sliding window to update forward and backward cumulative measures according to the state trellis with initial and ending states being determined by slight pilot symbols. Then, we select appropriate modulation parameters for the NRCPE based GMSK signaling according to the trade-offs of power and spectral efficiency [24]–[26]. Simulation results show that the proposed system can perform well even when suffering large Doppler shifts and high burst errors.

The main novelty and contribution of this paper are as follows.

- To eliminate error propagation existed in the RCPE, we design a non-recursive CPE (NRCPE) based on the Rimoldi's decomposition, whose output depends on the current and previous L input symbols.
- For improving the performance of the non-coherent demodulation and the impact of the Doppler shift in the coherent demodulation, we propose a pilot-aided quasi-coherent demodulation algorithm (PA-QCDA) based on the sliding-window technique.

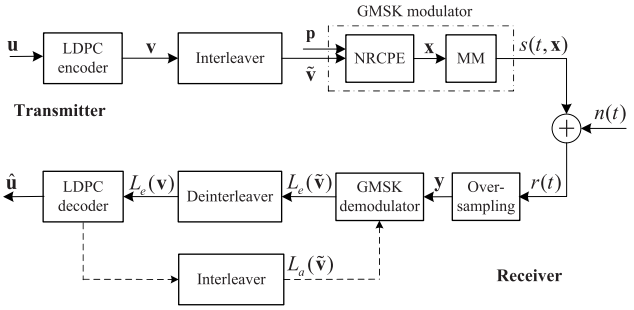

FIGURE 1. The block diagram of an LDPC coded GMSK system.

- Taking power and spectral efficiency into consideration, we select appropriate modulation parameters (e.g., h, L, B_gT) for the NRCPE-based GMSK signaling through the numerical analysis and Monte-Carlo simulation.

The remainder of this paper is organized as follows: In Section II, an LDPC coded NRCPE based GMSK system model is presented. In Section III, a pilot-aided quasi-coherent demodulation algorithm (PA-QCDA) is demonstrated. In Section IV, the modulation parameters for the NRCPE based GMSK signaling are chosen. Section V shows some simulation results and Section VI concludes this paper.

II. SYSTEM MODEL

A. LDPC CODED GMSK SYSTEM

Fig. 1 shows an LDPC coded NRCPE based GMSK system, where the GMSK modulator has a non-recursive structure using the Rimoldi's decomposition. Assume that a binary LDPC code $\mathcal{C}[N, K]$ of dimension K and length N is applied. At the transmitter, the input sequence of information symbols, $u = (u_0, u_1, \ldots, u_{K-1})$ with $u_i \in \{0, 1\}$, is first encoded by the LDPC encoder into a codeword $v = (v_0, v_1, \ldots, v_{N-1}) \in \mathcal{C}$ with $v_j \in \{0, 1\}$. The corresponding code rate is $R_{\mathcal{C}} = K/N$. After bit interleaving, the resulting codeword $\tilde{v} = (\tilde{v}_0, \tilde{v}_1, \ldots, \tilde{v}_{N-1})$ is appended with a length-W pilot sequence $p = (p_0, p_1, \ldots, p_{W-1})$, yielding a new sequence $c = (p, \tilde{v})$ of length $N_c = N + W$, whose structure is shown in Fig. 4. Next, the sequence c is mapped (natural mapping) to produce a M-ary sequence $d = (d_0, d_1, \ldots, d_{N_c-1}) \in \{\pm 1, \pm 3, \ldots \pm (M-1)\}$. For the GMSK modulation used here, we have $M = 2$ and thus $d = (d_0, d_1, \ldots, d_{N_c-1}) \in \{-1, +1\}$. According to the transform relation $a_i = (d_i + 1)/2 \in \{0, 1\}$, the sequence d is converted into another sequence $a = (a_0, a_1, \ldots, a_{N_c-1})$. By a non-recursive continuous-phase encoder (NRCPE) with memory length L, the sequence a is then encoded into an inner codeword $x = (x_0, x_1, \ldots, x_{N_c-1})$ with $x_k = (x_k^1, x_k^2, \ldots, x_k^{L+1})$, whose specific derivation is shown in Section II-B. Through a memoryless modulator (MM), the modulated signal waveform can be described by

$$s(t, x) = \sqrt{\frac{2E_s}{T}} \cos\left(2\pi f_c t + \bar{\phi}(t, x) + \phi_0\right), \qquad (1)$$

where E_s is the normalized symbol energy, T is the symbol duration, f_c is the carrier frequency, ϕ_0 is the initial phase,

and $\bar{\phi}(t, x)$ denotes the physical tilted-phase with the form of (when $t = \tau + kT$)

$$\bar{\phi}(\tau + kT, x_k) = [4\pi h \sum_{i=1}^{L} x_k^i q(\tau + (i-1)T) + 2\pi h x_k^{L+1} + \omega(\tau)] \mod 2\pi, \quad 0 \le \tau < T, \quad (2)$$

where $h \triangleq l/p$ is the modulation index (p and l are relatively prime integers), $q(t)$ is the Gaussian pulse response, and $\omega(\tau)$ represents the data-independent term with the form of

$$\omega(\tau) = \frac{\pi h \tau}{T} - 2\pi h \sum_{i=0}^{L-1} q(\tau + iT) + (L-1)\pi h. \quad (3)$$

Compared with the traditional phase based CPM, the titled-phase based one has a time-invariant state trellis with less states [20], which is helpful to reduce the demodulation complexity.

Finally, the modulated signal $s(t, x)$ is transmitted over an additive white Gaussian noise (AWGN) channel such that the received signal $r(t)$ is given by

$$r(t) = s(t, x) + n(t), \quad (4)$$

where $n(t)$ is the complex baseband AWGN with zero mean and one-side power spectral density of N_0.

At the receiver, the received signal $r(t)$ is first oversampled into a discrete sequence $y = (y_0, y_1, \ldots, y_{N_c-1})$ with a sampling period of T_s. Upon y, the GMSK demodulator computes log-likelihood ratio (LLR) $L_e(\tilde{v})$ for each bit in the sequence $\tilde{v}$ based on a modified BCJR algorithm. The resulting LLR $L_e(\tilde{v})$ are then de-interleaved and input to the LDPC decoder. Assume that the soft decision decoding algorithm is used for LDPC, the LDPC decoder can produce the *a posteriori* information intended for making hard decision to produce an estimate $\hat{u}$ of u. If considering the joint iterative scheme (see dashed lines in Fig. 1), the extrinsic information generated by the LDPC decoder is interleaved and sent back to the GMSK demodulator as the *a priori* information, denoted by $L_a(\tilde{v})$. Then, the GMSK demodulator uses y and $L_a(\tilde{v})$ to compute the LLR $L_e(\tilde{v})$. After de-interleaving, the resulting LLRs $L_e(v)$ are input to the LDPC decoder again. This process will stop if the maximum number of iterations is reached.

B. DESIGN OF THE NON-RECURSIVE CPE

In [20], Rimoldi has proved that any CPM modulator can be decomposed into a linear CPE with memory and a memoryless MM. According to the use of a modulo-p accumulator, the CPE can be classified as the recursive CPE (RCPE) and the non-recursive CPE (NRCPE) as shown in Fig. 2. Now, we will derive how to transform the RCPE into the desired NRCPE.

From Fig. 2(a), the output of the RCPE, x_k, can be defined as

$$x_k \triangleq \left(x_k^1, \ldots, x_k^L, x_k^{L+1}\right) = (a_k, \ldots, a_{k-L+1}, w_k), \quad (5)$$

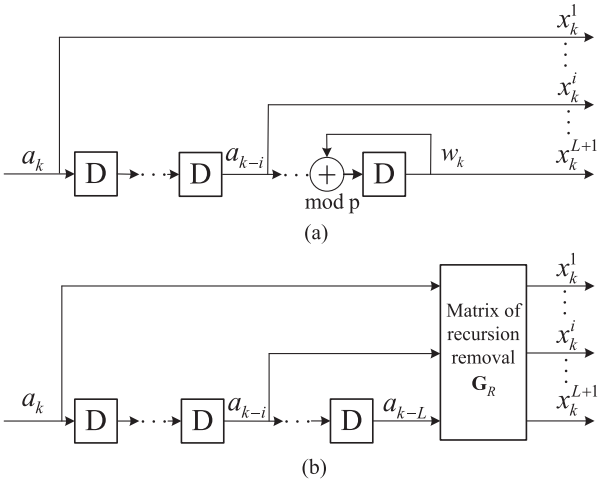

FIGURE 2. The CPE for GMSK modulation with memory length L. (a) RCPE. (b) NRCPE. Here, D denotes the delayer.

where a_k is the input symbol at time k, and w_k is the accumulated phase state at time k with the definition

$$w_k \triangleq \left[\sum_{k=0}^{k-L} a_k\right] \mod p. \quad (6)$$

Base on (6), the recursive relation of w_{k+1} to w_k can be transformed into the time shift relation of w_k to a_k, i.e.,

$$w_{k+1} = w_k + a_{k-L+1} \Rightarrow w_k = \frac{D^L}{1-D} a_k. \quad (7)$$

Thus, the output of the RCPE, x_k, can be rewritten as

$$x_k = a_k \left(1, D, \ldots, D^{L-1}, \frac{D^L}{1-D}\right). \quad (8)$$

In order to remove the recursive structure of the RCPE, it can be realized by multiplying both sides of (8) by $(1-D)$, i.e.,

$$(1-D)\, x_k = a_k \left(1 - D, D - D^2, \ldots, D^L\right). \quad (9)$$

In the light of Fig. 2(b), the output of the NRCPE, x_k, can be defined as

$$x_k \triangleq \left(x_k^1, x_k^2, \ldots, x_k^{L+1}\right) = (a_k, a_{k-1}, \ldots a_{k-L})\, G_R, \quad (10)$$

where G_R is called the matrix of recursion removal (RRM) with the dimension $(L+1) \times (L+1)$.

Then, assume that the results of (9) and (10) are equivalent, the specific form of the RRM can thus be deduced as

$$G_R = \begin{bmatrix} 1 & 0 & \cdots & 0 & 0 \\ -1 & 1 & \cdots & 0 & 0 \\ 0 & -1 & \cdots & 0 & 0 \\ \vdots & \vdots & \ddots & 1 & 0 \\ 0 & 0 & \cdots & -1 & 1 \end{bmatrix}_{(L+1)\times(L+1).} \quad (11)$$

TABLE 1. The parameter explanations used in Algorithm 1.

S_k	possible state	s_k	reference signal
α_k	forward cumulative measure	c_0	initial value of α_0 and β_0
β_k	backward cumulative measure	c_1	defined value of q_0
q_k	phase coherence measure	F_0	forgetting factor
γ_k	branch measure	F_1	modified factor
y_k	received signal	Λ	log probability

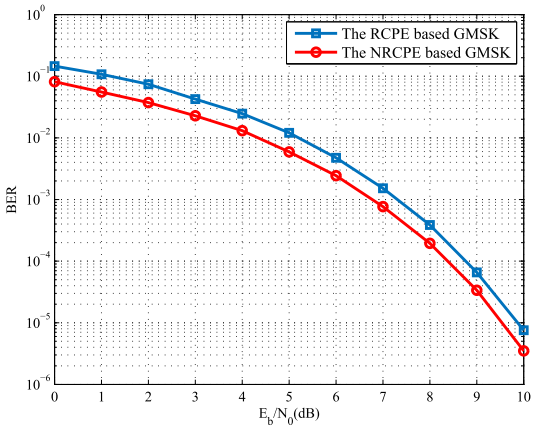

FIGURE 3. The BER results of the uncoded GMSK systems based on the RCPE and the NRCPE.

Finally, substituting (11) into (10) can obtain the actual output of the NRCPE, i.e.,

$$x_k = (a_k - a_{k-1}, \ldots, a_{k-L+1} - a_{k-L}, a_{k-L}) \mod p. \tag{12}$$

It can be concluded from (5)-(6) and (12) that the designed NRCPE depends only on the current and previous L input symbols instead of the current and all previous $k-1$ input symbols for the RCPE. Hence, the resulting NRCPE based GMSK system can eliminate the influence of the error propagation due to $k >> L+1$. Furthermore, the NRCPE based GMSK has MM^{L-1} states while the RCPE based one has pM^{L-1} states, thus achieving less states for small modulation index h (because $p >> M$, p is the denominator of the modulation index h).

To prove the superiority of the NRCPE over the RCPE, Fig. 3 shows the bit-error-rate (BER) performance of the uncoded GMSK systems based on the NRCPE and the RCPE. Simulation conditions are as follows: The length of information bits is 1024, the GMSK signaling is used over the AWGN channel with the modulation parameters $M = 2$, $h = 0.5$, $L = 2$ and $B_gT = 0.5$ (B_gT denotes the normalized 3 dB bandwidth of the Gaussian low-passing filter), and the Max-Log-MAP coherent demodulation algorithm is adopted [27]. It can be seen that the NRCPE based GMSK system can achieve better performance than the RCPE based one especially under the condition of low SNR, which implies that coded NRCPE based GMSK systems will be more competitive than coded RCPE based GMSK systems (see the blue and green curves in Fig. 6).

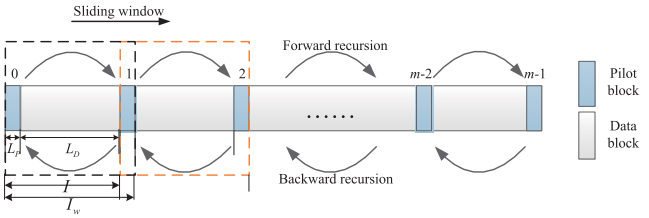

FIGURE 4. The schematic diagram of the PA-QCDA.

III. PILOT-AIDED QUASI-COHERENT DEMODULATION ALGORITHM (PA-QCDA)

Based on the classical pilot-symbol-assisted-modulation (PSAM) technique [28], we propose a modified BCJR detection algorithm, named pilot-aided quasi-coherent demodulation algorithm (PA-QCDA), where the sliding-window technique is applied as shown in Fig. 4. In Fig. 4, we set the distance between the two adjacent pilot blocks to a sliding window with the length of $I_w = L_D + 2L_P$, and the sliding interval is $I = L_D + L_P$, where L_D is the length of the data block and L_P is the length of the pilot block equal to the memory length L.

The basic idea of the PA-QCDA is using the received signals in each sliding window to update forward and backward cumulative measures according to the state trellis with initial and ending states being determined. For simplicity, we denote $q_k(S_k)$, $\alpha_k(S_k)$, $\beta_k(S_k)$ and $\gamma_k(S_k, S_{k+1})$ as q_k, α_k, β_k and γ_k, respectively. Table 1 lists all the assumed parameters for the PA-QCDA, whose specific operation steps are given in **Algorithm 1**. Note that if not using the pilot symbols, the PA-QCDA will be equivalent to a *non-coherent* demodulation algorithm.

In Table 1, the parameter F_0 is the forgetting factor to weaken the impact of the accumulated phase coherence measure, and the parameter F_1 is the modified factor to improve the demodulation performance, whose appropriate values can easily be found via Monte-Carlo simulations. Furthermore, when the existing Doppler shift is small, the value of q_0 we define, namely c_1, can also be found through Monte-Carlo simulations; otherwise, the value of q_0 is undefined and required to be computed by the received signals, which is helpful for the PA-QCDA to resist the large Doppler shift but with unnegligible performance loss. Hence, a joint

Algorithm 1 Pilot-Aided Quasi-Coherent Demodulation Algorithm (PA-QCDA)

for $i = 0, ..., m-2$ **do**
  //**initialization**
  $\alpha_{iI+0}(S_0 = 0) = c_0$
  $\beta_{iI+I-1}(S_{I-1} = 0) = c_0$
  $q_{iI+0}(S_0 = 0) = c_1$ *or undefined value*
  //**forward recursion start**
  for $k = 0, ..., I-1$ **do**
    $q_{iI+k+1} = F_0 \cdot q_{iI+k} + F_1 \cdot y_{iI+k} s^H_{iI+k}$
    $\gamma_{iI+k} = \left| q_{iI+k} + F_1 \cdot y_{iI+k} s^H_{iI+k} \right| - |q_{iI+k}|$
    $\alpha_{iI+k+1} = \max\limits_{S_{iI+k}} (\alpha_{iI+k} + \gamma_{iI+k})$
  end for
  //**backward recursion start**
  for $k = I-1, ..., 0$ **do**
    $\beta_{iI+k} = \max\limits_{S_{iI+k+1}} (\beta_{iI+k+1} + \gamma_{iI+k})$
  end for
  //**soft output calculation start**
  for $k = 0, ..., I-1$ **do**
    $\Lambda(\tilde{v}_{iI+k}) = \max\limits_{(S_{iI+k}, S_{iI+k+1})} (\alpha_{iI+k} + \gamma_{iI+k} + \beta_{iI+k+1})$
  end for
end for

demodulation and decoding iterative scheme will be required, as shown in Fig. 1.

IV. PARAMETER SELECTION OF THE NRCPE BASED GMSK SIGNALING

In order to select proper modulation parameters for the NRCPE based GMSK signaling, we need to evaluate the power spectral density (PSD) and spectral efficiency with respect to the parameters h, L and B_gT, given that $M = 2$. As illustrated in [20], the condition $M = p^k (k = 1, 2, 3...)$ should be satisfied for an arbitrary NRCPE based CPM system with a modulation index $h = l/p$.

The PSD can describe the power distribution over the bandwidth, a measure of power efficiency. Here, a correlation method is adopted to estimate the PSD for the NRCPE based GMSK signaling.

Specifically, we first calculate the correlation function $R(t, t+\tau)$ via averaging the product of the GMSK signal $s(t, x)$ and its delay signal $s(t+\tau, x)$, i.e.,

$$R(t, t+\tau) = E_x \{ s(t, x)\, s(t+\tau, x) \}. \tag{13}$$

Then, we compute the integral for (13) during the duration T and take the average, thus having

$$R(\tau) = \frac{1}{T} \int_0^T R(t, t+\tau)\, dt. \tag{14}$$

Taking the Fourier transformation for (14) can obtain the expected PSD, i.e.,

$$\Psi(f) = \mathcal{F}[R(\tau)] = \int_{\tau=-\infty}^{\infty} R(\tau) \exp(-j2\pi f \tau)\, d\tau. \tag{15}$$

Based on the above correlation method and Monte-Carlo simulations, the PSD of the NRCPE based GMSK signaling can be got. In simulations, we assume that $M = 2$, $h = 0.5$ and $L = 1/B_gT$ is various. Fig. 5 shows the PSD results of different NRCPE based GMSK signaling. Clearly, for $M = 2$ and $h = 0.5$, both the PSD curves of $L = 1/B_gT = 4$ and $L = 1/B_gT = 3$ are tighter and smoother than the case of $L = 1/B_gT = 2$. Therefore, it can be concluded that the larger L (i.e., the smaller B_gT), the tighter and smoother the corresponding PSD curve, but meanwhile the more serious the inter-symbol inference (ISI).

On the other hand, the capacity of the NRCPE based GMSK signaling over the AWGN channel can be estimated through Monte-Carlo simulations with the use of the BCJR algorithm [24]–[26]. Defining $I(x_0^{N_c-1}; y_0^{N_c-1})$ as the mutual information between the transmitted sequence $x = (x_0, x_1, \ldots, x_{N_c-1})$ and the received sequence $y = (y_0, y_1, \ldots, y_{N_c-1})$, the capacity of the NRCPE based GMSK signaling can be given by

$$\begin{aligned}
C &\triangleq \lim_{N_c\to\infty} \frac{1}{N_c} I(x_0^{N_c-1}; y_0^{N_c-1}) \\
&= \lim_{N_c\to\infty} \frac{1}{N_c} I(d_0^{N_c-1}; y_0^{N_c-1}) \\
&= \lim_{N_c\to\infty} \frac{1}{N_c} \left[H(d_0^{N_c-1}) - H(d_0^{N_c-1} | y_0^{N_c-1}) \right] \\
&= \lim_{N_c\to\infty} \frac{1}{N_c} \left[\sum_{i=0}^{N_c-1} \left(H(d_i | y_0^{i-1}) - H(d_i | y_0^{N_c-1}, d_0^{i-1}) \right) \right] \\
&= \log_2 M - \lim_{N_c\to\infty} \frac{1}{N_c} \sum_{i=0}^{N_c-1} E\left[\log_2 (p(d_i | y_0^{N_c-1}, d_0^{i-1})) \right] \\
&= 1 - \lim_{N_c\to\infty} \frac{1}{N_c} \sum_{i=0}^{N_c-1} E\left[\log_2 (p(d_i | y_0^{N_c-1}, d_0^{i-1})) \right],
\end{aligned} \tag{16}$$

where the term $p(d_i | y_0^{N_c-1}, d_0^{i-1})$ is computed by the BCJR algorithm, i.e.,

$$\begin{aligned}
p(d_i | y_0^{N_c-1}, d_0^{i-1}) &= p(S_i | y_0^{N_c-1}, S_0^{i-1}) \\
&= p(S_i | y_0^{N_c-1}, S_{i-1}) \\
&= \frac{\tilde{\beta}_i(S_i) \tilde{\gamma}_i(S_{i-1}, S_i)}{\sum\limits_{S_i} \tilde{\beta}_i(S_i) \tilde{\gamma}_i(S_{i-1}, S_i)},
\end{aligned} \tag{17}$$

where S_i is the state at the ith time instant, $\tilde{\beta}_i$ and $\tilde{\gamma}_i$ are calculated from the backward recursion, traversing all the state transitions at each time instant according to the standard procedure for the BCJR algorithm. Then, substituting (17) into (16) and calculating the expectation with the help of Monte Carlo simulations, the capacity C can be calculated. For spectral efficiency of the NRCPE based GMSK signaling, it can be defined as the ratio of the channel capacity C and the normalized bandwidth BT, i.e.,

$$\eta \triangleq \frac{C}{BT} \quad bit/s/Hz, \tag{18}$$

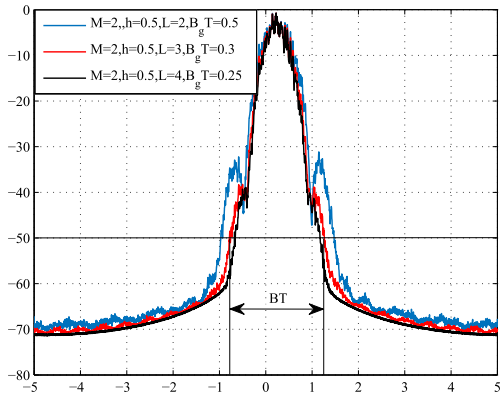

FIGURE 5. The PSD results of the NRCPE based GMSK signaling with various *h* and *L*.

TABLE 2. The modulation parameters of the NRCPE based GMSK signaling.

M	2	2	2
h	0.5	0.5	0.5
L	2	3	4
B_gT	0.5	0.3	0.25
BT	2.4	2.0	1.8
$\eta_{\max}$	0.42	0.50	0.56
$[E_b/N_0]_{thres}$	8	10	13

where BT is the normalized bandwidth corresponding to the bandwidth of the attenuation level of 50 dB in the PSD suggested by the Consultative Committee of International Radio (CCIR) 328-6 [29]. Clearly, when the SNR exceeds some threshold value, the capacity C can achieve the maximum value, i.e., 1 bit/symbol, and then η can approach to the maximum spectral efficiency.

Based on the above discussions, Table II lists the maximum spectral efficiency $\eta_{\max}$ and the SNR threshold $[E_b/N_0]_{thres}$ for different NRCPE based GMSK signaling, where the normalized bandwidth BT can be estimated from Fig. 5. It is shown that the NRCPE based GMSK signaling with larger L has lower SNR threshold but smaller spectral efficiency. Thus, the combination of $L = 3$ and $B_gT = 0.3$ is a compromising scheme. It is worth mentioning that the used memory length L is entirely determined by Monte Carlo simulations different from [30], where the memory length of the ISI can be adjusted by the packing ratio.

So far, the desired NRCPE based GMSK signaling can be determined by the parameters $M = 2$, $h = 0.5$, $L = 3$ and $B_gT = 0.3$.

V. SIMULATION RESULTS

In this section, we provide some simulation results to demonstrate the superiority of the proposed system. Assume that all the simulations are performed over the AWGN channel. We use a binary (3072,1024) LDPC code based on the fifth-generation (5G) LDPC code and a NRCPE based GMSK signaling with the parameters $M = 2$, $h = 0.5$, $L = 3$ and $B_gT = 0.3$. The sum-product algorithm (SPA) [31] is utilized to decode the LDPC code, and the PA-QCDA is adopted to detect the GMSK signals. In each sliding window, we suppose that $L_P = L = 3$ and $L_D = 32$, thus containing $3072/32 + 1 = 97$ pilot blocks. Accordingly, the rate loss (dB) caused by the pilot insertion can be estimated as

$$\begin{aligned} loss_P &= -10\log\left(1 - \frac{W}{N}\right) \\ &= -10\log\left(1 - \frac{97 \times 3}{3072}\right) \\ &\approx 0.4 \text{ dB}. \end{aligned}$$

Clearly, the larger the length of the data blocks L_D, the less the number of the pilot blocks, and thus the smaller the rate loss.

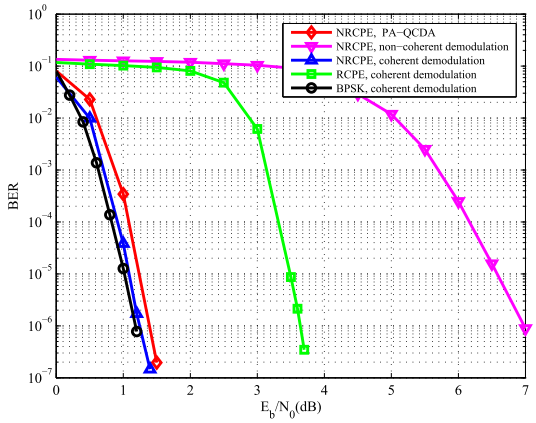

FIGURE 6. The BER results of the LDPC coded GMSK systems, where the RCPE and NRCPE based GMSK signaling is used with the PA-QCDA, non-coherent demodulation and coherent demodulation.

Fig. 6 compares the BER performance of the LDPC coded GMSK systems based on the NRCPE using the PA-QCDA, non-coherent demodulation and coherent demodulation (represented by the red, magenta and blue curves, respectively), and based on the RCPE using the coherent demodulation (represented by the green curve). The PA-QCDA uses a defined q_0, the non-coherent demodulation is a special case of the PA-QCDA, and the coherent demodulation uses the Max-Log-MAP algorithm. With the coherent demodulation applied, we observe that for BER $= 10^{-5}$, the NRCPE based system outperforms the RCPE based one by 3 dB, which proves the preceding analysis. For the above same BER, the LDPC coded NRCPE based GMSK system using the PA-QCDA can achieve only 0.3 dB performance loss relative to the LDPC coded BPSK system (represented by the black curve) and can obtain superior performance to the one using the non-coherent demodulation.

Considering the impact of burst errors on the LDPC coded NRCPE based GMSK system, we assume the parameter ε as the percentage of the continuous burst errors occurred in the received sequence. Based on the above simulation conditions, Fig. 7 compares the performance of the LDPC coded NRCPE

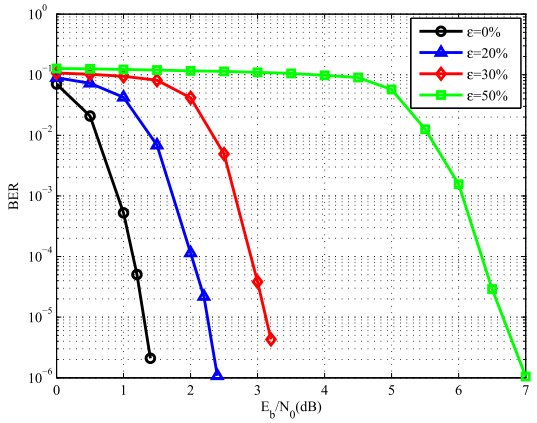

FIGURE 7. The BER results of the LDPC coded NRCPE based GMSK system using the PA-QCDA with different burst error proportions ε.

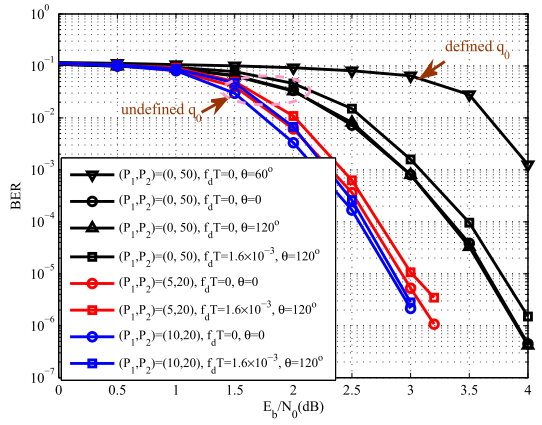

FIGURE 8. The BER results of the non-iterative and iterative LDPC coded NRCPE based GMSK system.

based GMSK system under different ε, where the PA-QCDA is used with a defined q_0. It is seen that for BER$= 10^{-5}$, the proposed system for $\varepsilon = 20\%$ and $\varepsilon = 30\%$ can achieve about 1 dB and 2 dB performance loss relative to that for $\varepsilon = 0\%$, respectively. As ε continues to grow, the corresponding performance loss will be unacceptable, which may be avoidable for the low-rate LDPC coded GMSK system.

Assuming there exist the Doppler shift f_dT and random phase offset θ, we consider the non-iterative-$(0, P_2)$ and iterative-(P_1, P_2) LDPC coded NRCPE based GMSK system, where P_1 and P_2 denote the number of the joint demodulation-decoding iteration and the solely decoding iterations, respectively. The PA-QCDA with the defined or undefined-q_0 is applied. Fig. 8 shows the corresponding performance comparisons. Clearly, the non-iterative-$(0, 50)$ system using the undefined-q_0 PA-QCDA can resist large Doppler shift and phase offset over that using the defined-q_0 PA-QCDA. For improving the performance of the iterative case, the P_1-joint iteration scheme with a practical P_2 is introduced. For $P_2 = 20$, the iterative system can obtain performance gain of 0.5 dB $\sim$ 1 dB at BER$= 10^{-5}$ when P_1 increases from 5 to 10.

VI. CONCLUSION AND FUTURE WORK

This paper presents an LDPC coded NRCPE based GMSK system for space communications. First, a matrix of recursive removal (RRM) is applied to the RCPE based GMSK modulator to alleviate the error propagation and reduce the number of phase states. Then, we propose a pilot-aided quasi-coherent demodulation algorithm (PA-QCDA) to improve the performance of non-coherent demodulation and resist the existing Doppler shift. Finally, some appropriate modulation parameters for the NRCPE based GMSK signaling are selected according to the trade-offs between the power and spectral efficiency via Monte-Carlo simulations. Simulation results show that the proposed system using the PA-QCDA can achieve excellent performance and perform well when suffering large Doppler shifts and random phase offsets or some burst errors.

In our future work, we will introduce the EXIT chart analysis and the asymptotic performance analysis into the LDPC coded GMSK system, which might be very helpful to improve the simulation results.

REFERENCES

[1] M. K. Simon, *Bandwidth-Efcient Digital Modulation With Application to Deep-Space Communications*. Sacramento, CA, USA: JPL Publication, 2001.
[2] M. Jia, X. Gu, Q. Guo, W. Xiang, and N. Zhang, "Broadband hybrid satellite-terrestrial communication systems based on cognitive radio toward 5G," *IEEE Wireless Commun.*, vol. 23, no. 6, pp. 96–106, Dec. 2016.
[3] J. B. Anderson, T. Aulin, and C.-E. Sundberg, *Digital Phase Modulation*. New York, NY, USA: Plenum Press, 1986.
[4] S. J. Maeng, H.-I. Park, and Y. S. Cho, "Preamble design technique for GMSK-based beamforming system with multiple unmanned aircraft vehicles," *IEEE Trans. Veh. Technol.*, vol. 66, no. 8, pp. 7098–7113, Aug. 2017.
[5] P. K. Sahoo, Y. K. Prajapati, and R. Tripathi, "PPM- and GMSK-based hybrid modulation technique for optical wireless communication cellular backhaul channel," *IET Commun.*, vol. 12, no. 17, pp. 2158–2163, Oct. 2018.
[6] G. M. A. Sessler, R. Abello, N. James, R. Madde, and E. Vassallo, "GMSK demodulator implementation for ESA deep-space missions," *Proc. IEEE*, vol. 95, no. 11, pp. 2132–2141, Nov. 2007.
[7] P. Moqvist and T. M. Aulin, "Serially concatenated continuous phase modulation with iterative decoding," *IEEE Trans. Commun.*, vol. 49, no. 11, pp. 1901–1915, Nov. 2001.
[8] P. Moqvist and T. Aulin, "Power and bandwidth efficient serially concatenated CPM with iterative decoding," in *Proc. IEEE Global Telecommun. Conf. (Globalcom)*, San Francisco, CA, USA, Nov./Dec. 2000, pp. 790–794.
[9] M. Xiao and T. M. Aulin, "Serially concatenated continuous phase modulation with convolutional codes over rings," *IEEE Trans. Commun.*, vol. 54, no. 8, pp. 1387–1396, Aug. 2006.
[10] D. Wang, G. Wang, and X. Xia, "An orthogonal space-time coded partial response CPM system with fast decoding for two transmit antennas," *IEEE Trans. Wireless Commun.*, vol. 4, no. 5, pp. 2410–2422, Sep. 2005.
[11] R. L. Maw and D. P. Taylor, "Space-time coded systems using continuous phase modulation," *IEEE Trans. Commun.*, vol. 55, no. 11, pp. 2047–2051, Nov. 2007.
[12] G. Wang, W. Su, and X.-G. Xia, "Orthogonal-like space–time-coded CPM systems with fast decoding for three and four transmit antennas," *IEEE Trans. Inf. Theory*, vol. 56, no. 3, pp. 1135–1146, Mar. 2010.
[13] R. G. Gallager, *Low-Density Parity-Check Codes*. Cambridge, MA, USA: MIT Press, 1963.
[14] D. J. C. MacKay, "Good error-correcting codes based on very sparse matrices," *IEEE Trans. Inf. Theory*, vol. 45, no. 2, pp. 399–431, Mar. 1999.
[15] M. Taki and M. B. Nezafati, "A new method for detection of LDPC coded GMSK modulated signals," in *Proc. Int. Conf. Wireless Commun., Netw. Mobile Comput.*, Wuhan, China, Sep. 2006, pp. 1–5.

[16] A. Kumar, R. Bahl, R. Gupta, and H. Choudhary, "Performance enhancement of GMSK and LDPC based VLF communication in atmospheric radio noise," in *Proc. Nat. Conf. Commun. (NCC)*, New Delhi, India, Feb. 2013, pp. 1–5.
[17] J. Bao, Y. Zhan, L. Yin, and J. Lu, "Design of efficient joint eIRA-coded MSK modulation systems for space communications," *IEEE Trans. Aerosp. Electron. Syst.*, vol. 48, no. 2, pp. 1636–1642, Apr. 2012.
[18] K. R. Narayanan and G. L. Stuber, "Performance of trellis-coded CPM with iterative demodulation and decoding," *IEEE Trans. Commun.*, vol. 49, no. 4, pp. 676–687, Apr. 2001.
[19] B. E. Rimoldi, "A decomposition approach to CPM," *IEEE Trans. Inf. Theory*, vol. IT-34, no. 2, pp. 260–270, Mar. 1988.
[20] L. Bahl, J. Cocke, F. Jelinek, and J. Raviv, "Optimal decoding of linear codes for minimizing symbol error rate," *IEEE Trans. Inf. Theory*, vol. IT-20, no. 2, pp. 284–287, Mar. 1974.
[21] R. Balasubramanian, M. P. Fitz, and J. V. Krogmeier, "Optimal and suboptimal symbol-by-symbol demodulation of continuous phase modulated signals," *IEEE Trans. Commun.*, vol. 46, no. 12, pp. 1662–1668, Dec. 1998.
[22] L. Yiin and G. L. Stuber, "Noncoherently detected trellis-coded partial response CPM on mobile radio channels," *IEEE Trans. Commun.*, vol. 44, no. 8, pp. 967–975, Aug. 1996.
[23] C.-H. Kuo and K. M. Chugg, "The capacity of constant envelope, continuous phase signals over AWGN channel under Carson's rule bandwidth constraint," in *Proc. IEEE Int. Conf. Commun. (ICC)*, May 2005, pp. 2179–2183.
[24] K. Padmanabhan, S. Ranganathan, S. P. Sundaravaradhan, and O. M. Collins, "General CPM and its capacity," in *Proc. IEEE Int. Symp. Inf. Theory (ISIT)*, Adelaide, SA, Australia, Sep. 2005, pp. 750–754.
[25] R. Chen, F. Wei, M. Huang, B. Li, and B. Bai, "On the capacity of CPM over Rayleigh fading channels," in *Proc. Int. Conf. Wireless Commun. Signal Process. (WCSP)*, Huangshan, China, Oct. 2012, pp. 1–5.
[26] W. Koch and A. Baier, "Optimum and sub-optimum detection of coded data disturbed by time-varying intersymbol interference," in *Proc. IEEE Global Telecommun. Conf. (Globecom)*, vol. 3, Dec. 1990, pp. 1679–1684.
[27] Y. Chen and N. C. Beaulieu, "Optimum pilot symbol assisted modulation," *IEEE Trans. Commun.*, vol. 55, no. 8, pp. 1536–1546, Aug. 2007.
[28] R. Kirby, "International standards in radio communication," *IEEE Commun. Mag.*, vol. 23, no. 1, pp. 12–17, Jan. 1985.
[29] Q. Shi, N. Wu, X. Ma, and H. Wang, "Frequency-domain joint channel estimation and decoding for faster-than-Nyquist signaling," *IEEE Trans. Commun.*, vol. 66, no. 2, pp. 781–795, Feb. 2018.
[30] F. R. Kschischang, B. J. Frey, and H.-A. Loeliger, "Factor graphs and the sum-product algorithm," *IEEE Trans. Inf. Theory*, vol. 47, no. 2, pp. 498–519, Feb. 2001.

HAI ZHU (M'19) received the Ph.D. degree from the School of Computer Science and Technology, Xidian University, Xi'an, China. He is currently an Associate Professor with the School of Network Engineering, Zhoukou Normal University. His research interests include information theory, LDPC coding, cloud computing, and the Internet of Things technology.

HENGZHOU XU (M'19) received the B.S. and M.S. degrees from the School of Mathematics and Statistics, Zhengzhou University, China, in 2009 and 2013, respectively, and the Ph.D. degree in communication and information system from Xidian University, China, in 2017. He is currently a Lecturer with the School of Network Engineering, Zhoukou Normal University, Zhoukou, China. His research interests include information theory, channel coding, and combinatorial designs.

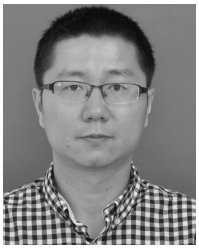

BO ZHANG received the B.S. and M.S. degrees from the Second Artillery Engineering College, Xi'an, China, and the Ph.D. degree from the School of Telecommunications Engineering, Xidian University, Xi'an. He is currently an Associate Professor with the School of Network Engineering, Zhoukou Normal University. His research interests include information theory, LDPC coding, capacity region, and transmission strategies for interference channels.

MENGMENG XU received the B.S. and M.S. degrees from the School of Mathematics and Statistics, Zhengzhou University, China, in 2009 and 2012, respectively, and the Ph.D. degree in communication and information system from Xidian University, China, in 2016. He is currently a Lecturer with the School of Network Engineering, Zhoukou Normal University, Zhoukou, China. His research interests include wireless ad hoc networks, resource allocation, routing design, and channel coding.

SIFENG ZHU received the Ph.D. degree from the School of Electronic Engineering, Xidian University, Xi'an, China. He is currently a Professor with the School of Network Engineering, Zhoukou Normal University. His current research interests include radio resource management in heterogeneous wireless networks and intelligent optimization algorithm.